Belgirate, Italy, 28-30 September 2005

MICROMACHINED HEAT EXCHANGER FOR A CRYOSURGICAL PROBE

Weibin Zhu[1], Yogesh B. Gianchandani[1], Gregory F. Nellis[2], Sanford A. Klein[2]
[1]University of Michigan, Ann Arbor, Michigan, USA
[2]University of Wisconsin, Madison, Wisconsin, USA

ABSTRACT

This paper describes a lithography-based microfabrication process developed for a recuperative heat exchanger intended for use in a cryosurgical probe. The probe, which uses the Joule-Thomson (JT) cooling cycle, must achieve a temperature < -50°C, with a freeze rate of 25-50°C/min. The heat exchanger must maintain high stream-to-stream thermal conductance while restricting parasitic stream-wise (axial) conduction losses. It has a footprint of 6x1.5cm^2 and 2.5mm thickness, and is fabricated using a five-mask process. Rows of fins composed of high conductivity silicon are bonded onto a 100μm base plate composed of low conductivity Pyrex glass. The fabrication process involves anodic bonding, deep reactive ion dry etching, glass frit bonding, electrochemical drilling and several other steps, along with special features that compensate for manufacturing tolerances. The paper describes the fabrication challenges and how they constrain dimensional variables.

I. INTRODUCTION

Cryosurgery is a medical procedure that is used to locally destroy cancerous tumors by exposing the pathological tissue to repeated freeze/thaw cycles [1]. The ablated tissue is subsequently allowed to thaw and is absorbed or sloughed by the body. By avoiding excision, operative blood loss and discomfort are minimized. Even in the cases where excision is required, pre-treatment of the tumor with cryotherapy can prevent the growth of tumor cells that might escape during resection. Cryosurgery has been used to treat several types of cancers in the past three decades, including prostate cancer and liver cancer.

For cancers located in easily accessible areas of the body, cryosurgical techniques have been a standard method of treatment that is competitive with other methods of therapy. Recent development of miniature cryoprobes with large refrigeration capacity [2-4] and techniques for real-time monitoring using ultrasound or magnetic resonant imaging [5-7] are allowing cryosurgical techniques to be applied to treatment of cancer in areas of body that are not readily accessible [8]. In fact, this effort, which examines the possible use of micromachining technology to fabricate cryoprobes, is motivated in part by the need to miniaturize cryoprobes to a size that permits them to be inserted through a small incision without loss of cooling power. The performance of the cyroprobe must not be compromised in this scaling effort. The region of cell death that surrounds the cold end of the probe is controlled by the refrigeration power and surface temperature attainable by the tip of the probe. It is known, for example, that temperatures below -50°C are always necrotic for pathological tissue [9-11]. In addition, a rapid cool-down rate [1, 12] between 25-50°C/min and multiple freeze-thaw cycles [13] are also preferred to decrease the cell survival.

The ultimate goal of this research effort is to develop a fully integrated micromachined cryosurgical probe that has significant advantages over the conventional cryosurgical probe in terms of thermal performance, size, flexibility and cost. The Joule-Thomson cooling cycle [14] can meet these requirements. In this cycle, cold, high-pressure fluid leaving a recuperative heat exchanger expands through a valve, resulting in a temperature drop through the valve if the state of the fluid lies below the inversion curve before expansion (Fig. 1). The probe has the potential for high reliability due to the absence of moving parts. This paper describes the design and fabrication of the micromachined recuperative heat exchanger for a Joule-Thomson cryosurgical probe. The

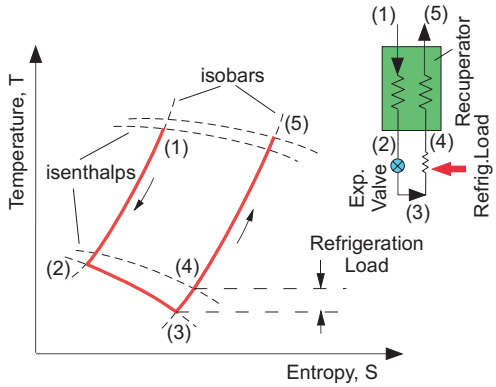

Fig. 1: Joule-Thomson refrigeration cycle. High pressure fluid at state (1) passes through a counter flow recuperator where it is pre-cooled by the low-pressure fluid returning from the refrigeration load. The cold high-pressure fluid leaving the recuperator at state (2) expands through a valve to state (3). The cold, low-pressure fluid is directed through the load heat exchanger where it is warmed by the refrigeration load to state (4) and then is fed back into the recuperator.

schematic diagram of this probe is shown in Fig. 2.

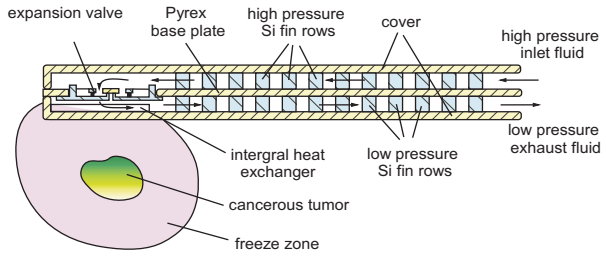

Fig. 2: Schematic diagram of micromachined Joule-Thomson cryosurgical probe. High pressure inlet fluid is obtained from an external compressor.

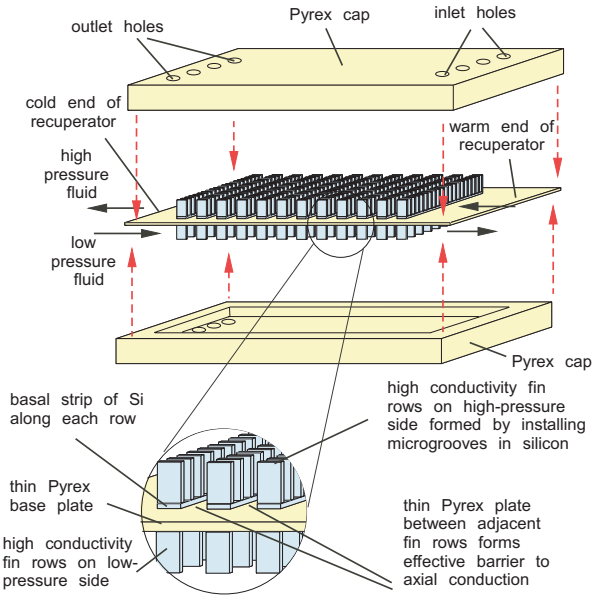

Fig. 3: Exploded schematic of the recuperator showing the magnified fin structure in an inset.

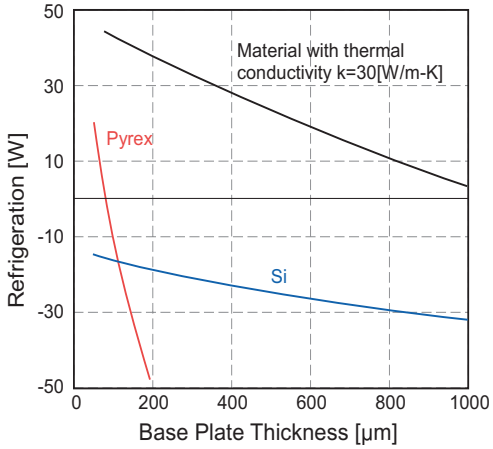

Fig. 4: Simulation results of cooling performance with different base plate materials and thickness. The system has positive refrigeration power with Pyrex base plate thickness no more than about 100µm.

II. DESIGN AND OPTIMIZATION

One of the critical challenges in developing a micromachined JT cooler is that the recuperative heat exchanger must maintain good stream-to-stream heat conductance while restricting parasitic stream-wise conduction losses. This requirement is necessary in order to have a large enthalpy difference between the two streams and thus achieve high cooling performance for the probe. The planar, micromachined recuperator in our design (Fig. 3) uses rows of fins that are composed of high conductivity silicon that is anodically bonded onto a very thin base plate composed of low conductivity Pyrex. This design is in contrast to conventional cryogenic heat exchangers that use either perforated plate designs with oxygen-free high conductivity (OFHC) copper plates interleaved with stainless steel spacers or finned tube designs which use one or more finned tubes wound on a mandrel. Silicon has thermal conductivity that is similar to OFHC copper, and Pyrex has thermal conductivity that is an order of magnitude less than stainless steel; this combination of very high and low thermal conductivity suggests that a silicon and Pyrex composite heat exchanger will be attractive.

However, in order to allow adequate thermal communication between the streams, preliminary modeling [15] and simulation (Fig. 4) of an optimized design [16] show that for a working pressure of 20 bar, the Pyrex base plate between the high pressure channel and low pressure channel can be no thicker than about 100µm in order to provide adequate refrigeration power. Because the base plate serves as an axial conduction barrier but is also part of the stream-to-stream thermal path a material with a conductivity that is intermediate between that of Pyrex and silicon would be optimal (around 30 W/m-K, as show in Fig. 4). However, initial prototypes have been fabricated using a Si-Pyrex-Si configuration.

III. FABRICATION

Several MEMS fabrication techniques, such as anodic bonding, deep reactive ion etching (DRIE) – which uses an inductively coupled plasma for alternating steps of etching and sidewall passivation, glass frit bonding, electrochemical drilling etc., are employed in the five masks fabrication process for the recuperative heat exchanger.

There are thirteen major steps included in this process (Fig. 5):

1) A Si-Pyrex-Si wafer stack is anodically bonded together. Because the Pyrex wafer is about 100µm thick, the bonding voltage is reduced to 500V. The entire stack is loaded simultaneously into the bonding apparatus and heated to 400°C, before the bonding voltage is applied.

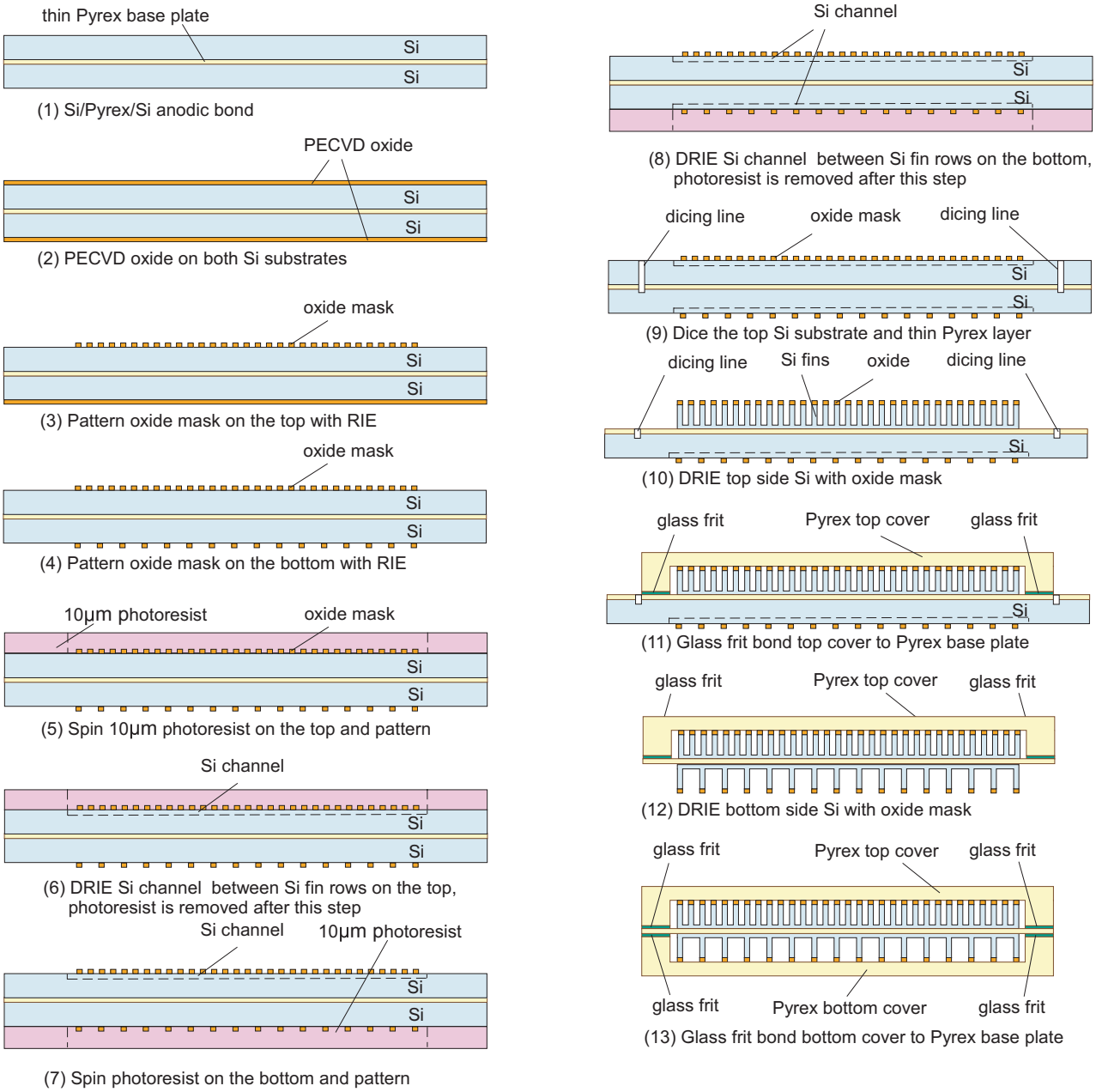

Fig.5: Fabrication process flow of micro recuperator.

By sequentially reversing the polarity of the voltage source, both Si-Pyrex interfaces are bonded one-by-one.

2) A 2μm-thick layer of silicon dioxide is deposited on both sides of the Si surface using plasma enhanced chemical vapor deposition (PECVD). This layer and a subsequent layer of photoresist will serve as masks in a two-step DRIE process.

3) The oxide layer on the high pressure (top) side is then patterned by reactive ion etching (RIE) using mixture of CF_4 and CHF_3.

4) A similar RIE step is utilized for patterning oxide mask on the low pressure (bottom) side.

5) A 10μm thick layer of photoresist is then coated and patterned on the top side. A conformal thick resist layer is used to protect the oxide pattern in next DRIE step.

6) Si channels between each fin rows are etched down 20μm on the top side by DRIE before the photoresist is stripped. This etch will ultimately lead to the creation of the basal strip along each row that is illustrated in the magnified part of Fig. 3. It is needed in part to compensate for a DRIE artifact that is explained below, but also has the added benefit of strengthening the attachment of the fins to the glass base plate.

7) A 10μm photoresist layer is coated and patterned on the bottom side.
8) Si channels between each fin rows are etched down 20μm on the bottom side with DRIE. The photoresist is then stripped.
9) The wafer is partially diced down to the Pyrex layer (300μm deep). The purpose of this step is to ensure that the device automatically separates in the final DRIE step (step 12) on the bottom side.
10) Fin rows on the top side are etched and defined by DRIE with oxide mask. This is a high aspect ratio etch of 180μm depth. It must clear the narrow regions between rows, etch between the tightly packed fins, but it also has to clear the perimeter of the device, which has no masked features, and etches faster.

Optimizing the DRIE chemistry is one of the significant challenges of the process for three reasons: (a) the relatively large size of the device and the narrow widths of the fins demands high uniformity over a large area; (b) the DRIE step must clear the narrow openings between rows and the wide spaces of the perimeter simultaneously; and (c) the termination of the etch on the glass layer sandwiched between the two Si layers causes etching ions to be deflected due to charge build-up in the glass. This last effect leads to a problem known as "footing," which is the lateral spread of the etch profile once the insulating glass is exposed at the bottom of the trench [17]. The two-step DRIE (in steps 6 and 10) is necessary to fabricate separated grooves on the high-pressure side, shown in Fig. 3, and compensate for the non-uniform etch rate due to the varying density of the features. Due to the micro loading effect [18, 19], the areas between fins and fin rows with small openings are usually etched more slowly than the area around the device with large openings. In order to achieve high performance, each fin row must be thermally isolated along the flow direction. Therefore, the Si in the gap between fin rows must be completely etched away while the over-etch in the area around the device must be minimized to prevent the footing effect from damaging the fins close to those areas. In step 6, the area between each fin row is etched down 20μm, allowing this densely packed region to be etched through fully during the DRIE in step 10.
11) A glass cap (the fabrication of which is described separately, below) is bonded to the base plate with commercial glass frit tape (G1017, from Vitta Corp.) at 500°C so as to construct a sealed chamber on the high pressure side. A significant challenge in this step is the patterning the tape, which cannot be done lithographically. In this effort, because of the large bonding area of this device, the tape could be manually cut and placed on each die.
12) A similar DRIE process is completed on the low-pressure side afterward. The devices are separated in this step because the silicon underneath the dicing line is removed.
13) Another glass cap is bonded onto the bottom side of base plate using glass frit.

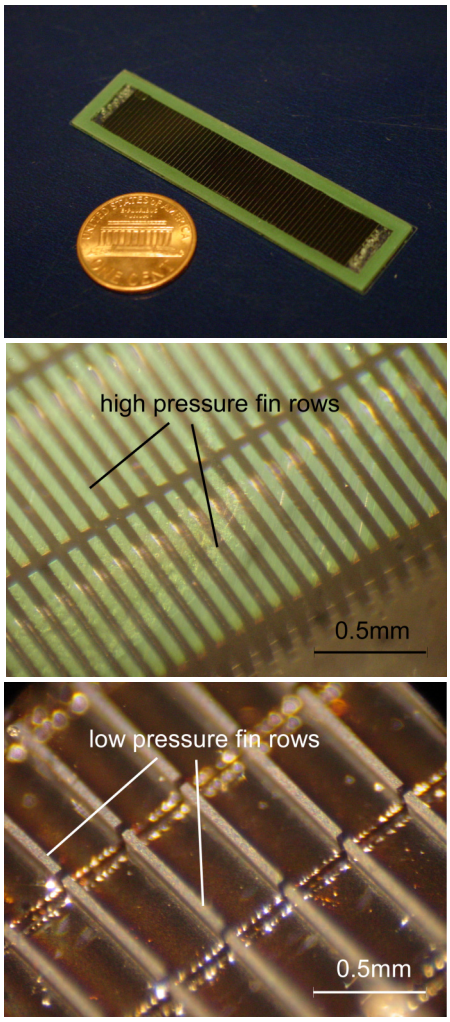

Fig. 6: a) The size of micro recuperator is 6cm×1.5cm with total 2.5mm thickness. Gap between each fin row is 51μm. b) High pressure fin rows with 50μm gap. Fin size is 50μm×782μm, 200μm high. c) Low pressure fin rows with 345μm gap. Fin size is 50μm×782μm, 200μm high.

Glass Cap Fabrication:

The glass caps are fabricated from 1.1 mm thick Pyrex wafers. The Pyrex wafer is coated with 500Å/5000Å Cr/Au layer and then patterned with photoresist. Using the metal layer as a mask, the wafer is immersed in the HF:HNO_3 solution to create a recess that is 100μm deep. The photoresist and Cr/Au layer are removed after the wet etching. Inlet and outlet holes are drilled with electrochemical discharge drilling method [20]. This method provides a smooth and debris-free surface, but is a serial method, and is not performed

lithographically. An electrode wire is positioned in the proximity of the glass wafer while both are immersed in NaOH 30% wt. solution at room temperature. A bias of 33V permits a 1100μm thick glass plate to the perforated in about 10s. The wafer is finally diced into several glass caps.

Figure 6 shows a fabricated micro recuperative heat exchanger. The size of this device is 6cm×1.5cm with 2.5mm total thickness.

IV. CONCLUSIONS

In addition to the challenges in the various steps identified in the preceding section, the development of the fabrication process has yielded a number of important lessons. At a very basic level, the fragility of the 100μm thick glass plate requires that it be bonded to at least one Si wafer as early in the process as possible. Another general challenge is the footprint of the device, which is so large that the possibility of a defect or non-uniformity is high. In the processing steps, as already discussed, the primary challenges include the double-sided bonding of the glass wafer; the DRIE sequence and its limitations related to overall uniformity, micro loading, and footing; the frit glass bonding; and the electrochemical etching. However, reasonable solutions exist for each of these challenges, and a feasible process for manufacturing heat exchangers in this manner has been developed.

Preliminary tests show that the recuperative heat exchanger has no significant leakage on both sides under high pressure flow. The cooling performance of this device is currently being tested over a range of pressures and temperatures and will be compared with the model predictions. In the long term, this device will include temperature sensors and auxiliary heaters for sensing and controlling freeze zone. The robustness, flexibility and performance associated with the micromachined device may result in the application of cryosurgery to new biomedical areas.

ACKNOWLEDGEMENTS

The authors thank Mr. Michael Frank for his effort in modeling and optimizing the dimensions of the heat exchanger. This work was funded in part by a grant from the US National Institutes of Health (R21 EB003349-02).

REFERENCES

[1] J. Dobak, "A Review of Cryobiology and Cryosurgery," *Advances in Cryogenic Eng.*, 43, pp. 889-896, 1998.

[2] Z. H. Chang, J. J. Finkelstein, and J. G. Baust, "Optimization of Cryosurgical Instrumentation for use in Minimally Invasive Prostate Surgery," in *Recent Advances in Cryogenic Engineering*, J.P. Kelley and J. Goodman, eds., ASME, New York, pp. 45-55, 1993.

[3] B. Z. Maytal, "Fast Joule-Thomson Cryocycling Device for cryosurgical Applications," *Advances in Cryogenic Engineering*, 43, pp. 911-917, 1998.

[4] J. Dobak, X. Yu, and K. Ghaerzadeh, "A Novel Closed Loop Cryosurgical Device," *Advances in Cryogenic Engineering*, 43, pp. 897-902, 1998.

[5] R. Masumoto, K. Oshio, F.A. Jolesz, "Monitoring of Laser and Freezing-Induced of the Liver with Tl-Weighted MR Imaging," *J. Magnetic Resonance Imaging*, 2, pp. 555, 1992.

[6] B. Rubinsky, J.C. Gilbert, G.M. Onik, M.S. Roos, S.T. Wong, K.M. Brennan, "Monitoring Cryosurgery in the Brian and Prostate with Proton NMR," *Cryobiology*, 30, pp. 191-199, 1993.

[7] G.R. Pease, S.T. Wong, M.S. Roos, B. Rubinsky, "MR Image-Guided Control of Cryosurgery," *Journal of Magnetic Resonance Imaging*, 5, pp. 753-760, 1995.

[8] J. K. Cohen, R.J. Miller, "Thermal Protection of Urethra during Cryosurgery of the Prostate," *Cryobiology*, 31, pp. 313-316, 1994.

[9] A. Gage, "Five-year Survival Following Cryosurgery for Oral Cancer," *Archives of Surgery*, 111, pp. 990-994, 1976.

[10] A.A. Gage, J.A. Caruana and M. Montes, "Critical Temperature for Skin Necrosis in Experimental Cryosurgery," *Cryobiology*, 19, pp. 273-282, 1982.

[11] J. Bischoff, K. Christov, B.A. Rubinsky, "Morphological Study of Cooling Response in Normal and Neoplastic Human Liver Tissue: Cryosurgical Implications," *Cryobiology*, 30, pp. 482-492, 1993.

[12] A.A. Gage, K. Guest, M. Montes, J.A. Caruana, D. A. Whalen, Jr., "Effect of Varying Freezing and Thawing Rates in Experimental Cryosurgery," *Cryobiology*, 22, pp. 175-182, 1985.

[13] A.A. Gage, "Cryosurgery in the Treatment of Cancer," *Surgery, Gynecology & Obstetrics*, 174, pp. 73-92, 1992.

[14] E.D. Marquardt, R. Radebaugh, J. Dobak, "A cryogenic Catheter for Treating Heart Arrhythmia," *Advances in Cryogenic Engineering*, 43, pp. 903-910, 1998.

[15] G. F. Nellis, "A Heat Exchanger Model that Includes Axial Conduction, Parasitic Heat Load, and Property Variations," *Cryogenics*, Vol. 43, No. 9, pp. 523-538, 2003.

[16] M. Frank, M, *Recuperative Heat Exchanger for a MEMS Cryoprobe*, M.S. Thesis, Univ. Wisconsin, Mechanical Engineering Dept., (2004).

[17] K. Ishihara, C.F. Tung, A.A. Ayón, "An Intertial Sensor Technology Using DRIE and Wafer Bonding with Interconnecting Capability," *J. Microelectromechanical Systems*, Vol. 8, No. 4, pp. 403-408, 1999.

[18] K. Kühl, S. Vogel, U. Schaber, R. Schafflik, B. Hillerich, "Advanced Silicon Trench Etching in MEMS Applications," *SPIE*, Vol. 3511, Santa Clara, California, pp. 97-105, 1998.

[19] M. Chabloz, J. Jiao, Y. Yoshida, T. Matsuura, K. Tsutsumi, "A Method to Evade Microloading Effect in Deep Reactive Ion Etching for Anodically Bonded Glass-silicon Structures," *IEEE Intl. Conf. on Micro Electro Mechanical Systems (MEMS'00)*, Miyazaki, Japan, pp. 283-287, 2000.

[20] V. Fascio, R. Wüthrich, D. Viquerat, H. Langen, "3D Microstructuring of Glass Using Electrochemical Discharge Machining (ECDM)," *International Symposium on Micromechatronics and Human Science*, pp. 179-183, 1999.